Research Article Vol. 1, No. 3 / September 2014 / Optica 158

CW-pumped single-pass frequency comb generation by resonant optomechanical nonlinearity in dual-nanoweb fiber

A. Butsch,* J. R. Koehler, R. E. Noskov, and P. St.J. Russell

Max Planck Institute for the Science of Light, Guenther-Scharowsky-Str. 1, 91058 Erlangen, Germany

**Corresponding author: anna.butsch@mpl.mpg.de*

Received 23 May 2014; revised 6 August 2014; accepted 6 August 2014 (Doc. ID 212716); published 10 September 2014

Recent experiments in the field of strong optomechanical interactions have focused on either structures that are simultaneously optically and mechanically resonant, or photonic crystal fibers pumped by a laser intensity modulated at a mechanical resonant frequency of the glass core. Here, we report continuous-wave (CW) pumped self-oscillations of a fiber nanostructure that is only mechanically resonant. Since the mechanism has close similarities to stimulated Raman scattering by molecules, it has been named stimulated Raman-like scattering. The structure consists of two submicrometer thick glass membranes (nanowebs), spaced by a few hundred nanometers and supported inside a 12-cm-long capillary fiber. It is driven into oscillation by a CW pump laser at powers as low as a few milliwatts. As the pump power is increased above threshold, a comb of Stokes and anti-Stokes lines is generated, spaced by the oscillator frequency of ~6 MHz. An unprecedentedly high Raman-like gain of $\sim 4 \times 10^6$ m^{-1} W^{-1} is inferred after analysis of the experimental data. Resonant frequencies as high as a few hundred megahertz are possible through the use of thicker and less-wide webs, suggesting that the structure can find application in passive mode-locking of fiber lasers, optical frequency metrology, and spectroscopy.

OCIS codes: (200.4880) Optomechanics; (190.5890) Scattering, stimulated; (060.4005) Microstructured fibers; (190.4370) Nonlinear optics, fibers.

http://dx.doi.org/10.1364/OPTICA.1.000158

1. INTRODUCTION

In recent years, a major thrust in optomechanics has been the observation of light–matter interactions at the single quantum level [1,2]. Remarkable microstructures have been developed in which both light and acoustic vibrations are tightly confined within a small volume for relatively long periods of time, and thus forced to interact strongly. An extensive review of the recent progress in this field can be found in [3].

Another goal of optomechanics has been the design of micro/nanostructures that display very high optomechanical nonlinearities, through either electrostrictive changes in refractive index [4,5] or radiation-pressure-driven changes in morphology [6,7]. For example, in small-core silica–air photonic crystal fibers, it has been shown that acoustic core resonances at few-gigahertz frequencies can be excited electrostrictively by pumping with dual-frequency laser light [8]. These core resonances then act back on the light, resulting in the generation of an optical frequency comb. This process, which was named stimulated Raman-like scattering (SRLS), has been used to passively mode lock a fiber ring laser at gigahertz frequencies [9].

Another example is the dual-nanoweb fiber (the subject of this work), a structure that displays a giant optomechanical nonlinearity as a result of the high mechanical compliance of two very thin, wide, and closely spaced glass "nanowebs" mounted inside a fiber capillary [see Fig. 1(a)] [10]. When light of only a few milliwatts is launched into the nanowebs so that the phase across them is constant (i.e., the even mode is excited), optical gradient forces cause the webs to be pulled

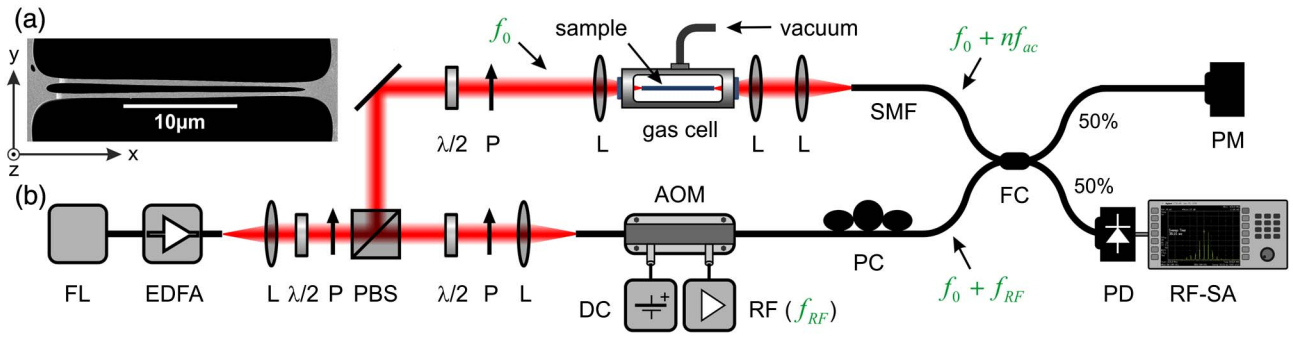

Fig. 1. (a) Scanning electron micrograph of the fiber core region: the width w of the dual-nanoweb waveguide is ~22 μm, the upper and lower web thicknesses in the center are $h_u \sim 460$ nm and $h_l \sim 480$ nm, and the gap thickness is $h_g \sim 550$ nm. The sample length L is 12 cm. (b) Schematic of the heterodyne detection setup with an evacuated dual-nanoweb fiber sample. FL, fiber laser; EDFA, erbium-doped fiber amplifier; L, lens; P, polarizer; PBS, polarizing beam splitter; AOM, acousto-optical modulator; SMF, single mode fiber; PC, polarization controller; FC, fiber coupler; PD, photodiode; RF-SA, radio-frequency spectrum analyzer; PM, power meter.

together, increasing the effective index of the mode. If the odd mode is instead excited, the webs are pushed apart, but the modal index still rises [11].

In a previous study, the frequency response of this nonlinearity was measured at different gas pressures [12]. When driven by a laser beam intensity-modulated at the frequency of the fundamental flexural resonance of the nanowebs, effective optomechanical nonlinearities ($m^{-1}\,W^{-1}$) some 60,000 times higher than the Kerr-related nonlinearity were measured.

Something more intriguing is observed, however, when the gas pressure is reduced to the μbar range (thus eliminating viscous damping and squeezed-film effects) and the structure is pumped with CW light. Above a sharp threshold of a few milliwatts, the output signal begins to oscillate in intensity and sidebands appear in the optical frequency spectrum [13]. Unlike in previous experiments with CW light where optical cavities with high Q factors (for example, in highly nonlinear fibers [14] or whispering gallery mode resonators [15]) were used to generate frequency combs via the electronic Kerr effect, the underlying mechanism in our case is SRLS. As we will show, this effect is initiated by scattering of light at thermally excited phonons. This gives rise to weak uncorrelated Stokes (S) and anti-Stokes (AS) signals. For certain combinations of the randomly fluctuating phases of these signals, the beat note with the pump light drives the acoustic resonance more strongly, further enhancing scattering into the sidebands. An optical frequency comb spaced by the acoustic resonant frequency (~6 MHz) is created. Symmetry between S and AS scattering causes suppression of pump-to-Stokes Raman gain in gases in the special case when both S and AS are phase-matched to the same coherence wave [16]. In our case, however, because of the much stronger thermal vibrations at 6 MHz (kT-driven molecular excitations are vanishingly weak at the multiterahertz frequencies typical of gases) enhanced by the high mechanical Q factor, a substantial population of stochastic thermal phonons is available to stimulate Stokes photon creation, or to cause frequency up-shifting to the anti-Stokes. As a result, no gain suppression is seen.

Here, we report in detail on this new phenomenon, which can be viewed as the first example of noise-seeded, optomechanical SRLS; the dual-nanoweb structure behaves like a sort of "artificial Raman-active molecule."

2. STRUCTURE, SETUP, AND EXPERIMENTAL RESULTS

The ~22 μm wide waveguide region of the dual-nanoweb fiber consists of two optically coupled nanowebs with slightly convex thickness profiles. The thicknesses of the upper and lower nanowebs are ~460 nm and ~480 nm at the center, and the gap between them is ~550 nm wide [Fig. 1(a)]. In the experiment, a 12 cm long sample was used, mounted in a gas cell with windows at each end and evacuated to a pressure of ~1 μbar. This strongly enhanced the Q factor of the acoustic vibrations and the strength of the resonant optomechanical nonlinearity [12]. As explained above, the system began oscillating when a few milliwatts of CW laser light at 1550 nm was launched into the fiber [13]. The resulting RF spectrum was measured with high resolution using the heterodyne setup depicted in Fig. 1(b).

The laser system comprised a narrow-linewidth single-mode fiber laser (3 dB linewidth ~3 kHz) and an erbium-doped fiber amplifier (EDFA). Using a combination of $\lambda/2$ plate and polarizer before and after the polarizing beam splitter, the power and polarization state in both the sample and the local oscillator (LO) paths could be controlled. TE-polarized light was launched into the sample and the transmitted signal, containing the pump and the optomechanically created sidebands, was coupled into a single mode fiber and mixed with the LO signal at a fiber coupler. In the LO path, an acousto-optical modulator was used to upshift the optical carrier frequency by 200 MHz. The beat note between the signals transmitted through the sample and LO path was then detected using a fast photodiode and visualized using a radio-frequency spectrum analyzer. The RF power P_n^{RF} of the beat note between the nth comb component with power P_n and the LO with power P_{LO} is proportional to the product of both optical powers, i.e., $P_n^{\mathrm{RF}} \propto P_n P_{\mathrm{LO}}$ [17].

In Fig. 2, a series of four RF spectra are shown, measured at different launched pump powers P_{IN} and constant P_{LO}, the RF power therefore being proportional to the optical power

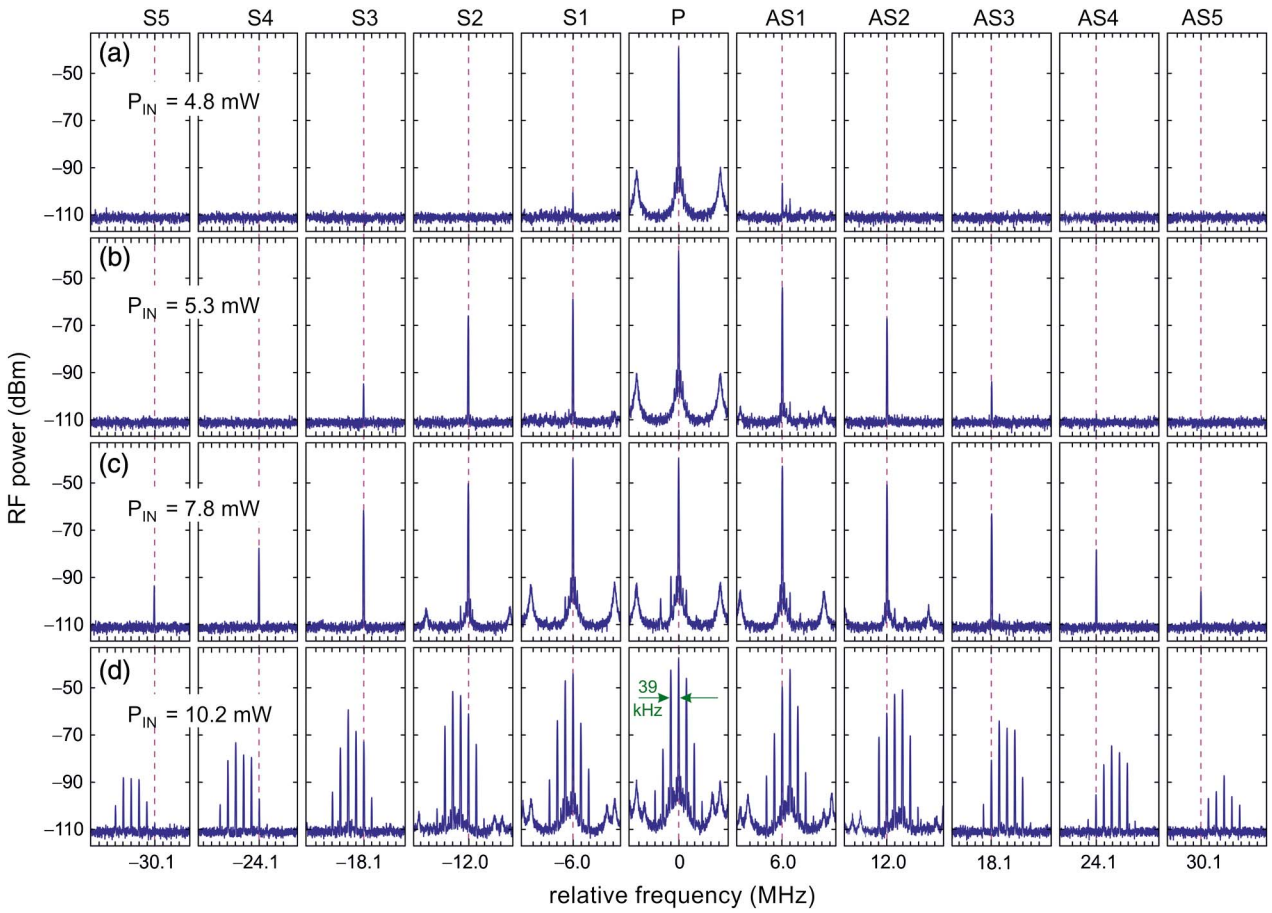

Fig. 2. RF spectra of the transmitted optical signal measured at different CW input powers. The frequency was scanned over 500 kHz around each of the comb sidebands at multiples of ±6.022 MHz. (a) Initial amplification of first-order S and AS components at 4.8 mW input power. (b) At 5.3 mW, three sidebands appear on each side of the pump peak. (c) S and AS components up to fifth order are detected at 7.8 mW input power. (d) At 10.2 mW, a fine structure of lines with a spacing of 39 kHz appears around each of the main comb components. The tick spacing on the frequency axis of each pane is 39 kHz.

of the corresponding comb component. Note that the laser system exhibits sidebands at ±210 kHz relative frequency, which are, however, suppressed by more than 53 dB relative to the main laser line and cannot seed any optomechanical sidebands due to the frequency mismatch. The spectrum at 4.8 mW exhibits, on either side of the pump peak (at zero relative frequency and ∼70 dB above the background noise), small S and AS peaks (∼10 dB above the noise level) at ±6.022 MHz, corresponding to the fundamental flexural resonance of the structure. As the input power is increased to 5.3 mW, six sidebands spaced by 6.022 MHz can already be distinguished. At 7.8 mW, the number of sidebands increases to ten. When the launched power is raised above ∼8 mW, a fine structure of the comb lines with a frequency spacing of 39 kHz appears, and at 10.2 mW, four to six secondary comb lines can be observed around each of the main peaks. When the air pressure inside the fiber is increased to a few mbar, viscous damping of the flexural vibrations causes the threshold power for the onset of comb generation to rise considerably, until above ∼100 mbar it is no longer possible to generate a frequency comb at the power levels available in the experiment.

To further characterize the system, we measured the SRLS gain spectrum using the copolarized dual-frequency (pump+S) excitation technique [8]. This involved inserting an electro-optic modulator driven by a function generator before the EDFA, its DC bias adjusted so that two equal amplitude sidebands are synthesized and the carrier wave strongly suppressed.

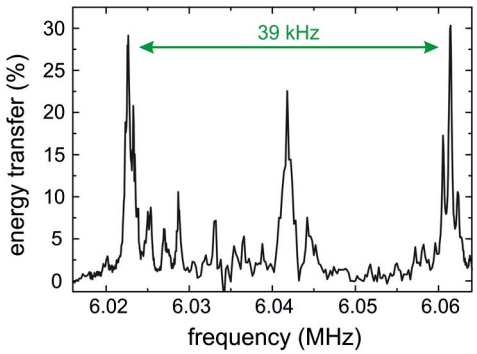

Fig. 3. Energy transfer from pump to Stokes as a function of the frequency spacing of the dual-frequency light (50% pump and 50% Stokes) at 2 mW launched total power.

Figure 3 shows the energy transfer from the pump to the S wave, after propagation through the dual-web fiber, as a function of the frequency spacing between them. The total launched power level was kept at a low ~2 mW so as to minimize conversion to higher-order sidebands. Interestingly, the spectrum reveals clusters of closely spaced sharp peaks, similar to those observed previously [12]. These peaks we attribute to flexural resonances localized at structural nonuniformities along the fiber sample. Two distinct resonances appear at 6.022 and 6.061 MHz, spaced 39 kHz and, as we will show later, the interaction between these resonances leads to the generation of the fine structure of the comb lines.

3. MECHANISM AND THEORY

In this section, we set up a theoretical model for the noise-initiated SRLS and determine its gain characteristics. We restrict the analysis to the lowest-order TE-polarized optical mode [single-lobed in the y and x directions, Fig. 1(a)] and the fundamental acoustic flexural mode (single-lobed in the x direction) [10]. The flat dispersion curve of the flexural mode and the small frequency shift (cut-off frequency ~6 MHz) ensure that the same phonon can cause phase-matched coupling between successive S and AS components (Fig. 4). This means that the model must take into account a large number of comb components, spaced by ~6 MHz.

The nonlinear wave equation for the electric field may be written as [8]

$$\frac{\partial^2 E}{\partial z^2} - \frac{n_m^2}{c^2}\frac{\partial^2 E}{\partial t^2} = \frac{1}{\varepsilon_0 c^2}\frac{\partial^2 P_{\mathrm{NL}}}{\partial t^2}, \tag{1}$$

where the nonlinear polarization P_{NL} describes the coupling between optical and acoustic fields. The refractive index of the optical mode is n_m, ε_0 is the dielectric permittivity, and c is the speed of light *in vacuo*. The optomechanical nonlinearity originates from the interdependence of optical gradient forces and deflection-dependent changes in n_m, and strongly dominates over the contributions of photoelasticity and electrostriction, which we therefore neglect. P_{NL} can therefore be expressed to first order as [18]

$$P_{\mathrm{NL}} = \varepsilon_0 \frac{\partial \varepsilon}{\partial \delta}\delta E = 2\varepsilon_0 n_m \frac{\partial n_m}{\partial \delta}\delta E. \tag{2}$$

The web deflection δ is governed by the flexural wave equation for a thin plate [19,20]:

$$D\left(1+\tau\frac{\partial}{\partial t}\right)\left(\frac{\partial^4\delta}{\partial x^4}+2\frac{\partial^4\delta}{\partial x^2\partial z^2}+\frac{\partial^4\delta}{\partial z^4}\right)+\sigma\frac{\partial^2\delta}{\partial t^2} = p_{\mathrm{opt}}+\tilde{f}\approx\frac{\varepsilon_0}{2}[E^2]_{y=y_{\mathrm{lower}}}^{y=y_{\mathrm{upper}}}+\tilde{f}, \tag{3}$$

where $D = Yh^3/[12(1-\nu^2)]$ is the flexural rigidity of a nanoweb with thickness h, Y is the Young's modulus, and ν is the Poisson's ratio. The parameter τ is related to the damping rate (see below). The driving term is given by the optical gradient pressure p_{opt}, which can be calculated using the Maxwell stress tensor [11]. To simplify the analysis, we neglect magnetic field components (they contribute only ~6% to the interweb force) and approximate p_{opt} acting on one web by evaluating the difference between the squared electric fields at its upper and lower surfaces [18]. Further, in Eq. (3), we have introduced a Langevin noise source $\tilde{f}$ describing the thermal excitation of acoustic waves, based on δ-correlated Gaussian noise [21].

Assuming that the fiber has no structural nonuniformities along its length, the electric field, containing an infinite number of copolarized equidistant-in-frequency components, can be written in the form

$$E(x,y,z,t) = s(x)f(y)\sqrt{\frac{P_0 Z_0}{2n_m}}\sum_n a_n(z,t)e^{i(\beta_n z-\omega_n t)} + \text{c.c.}, \tag{4}$$

where Z_0 is the impedance of vacuum, P_0 is the launched optical power, and $s(x)f(y)$ represents the transverse field distribution of the optical mode, normalized so that $\int_{-w/2}^{w/2}|s(x)|^2\mathrm{d}x = 1$ and $\int_{-\infty}^{\infty}|f(y)|^2\mathrm{d}y = 1$. For the structures studied here, $s(x)f(y)$ can be taken to be independent of power for launched powers in the milliwatts range [10]. Within this normalization, $s(x)$ and $f(y)$ have units $\mathrm{m}^{-1/2}$. The dimensionless functions $a_n(z,t)$ represent the slowly varying field amplitudes of the comb lines, with frequency $\omega_n = \omega_0 + n\Omega$ and axial propagation constant $\beta_n = \beta_0 + nq$, where ω_0 is the angular frequency, β_0 is the wavevector of the pump mode, and $n = \pm1, \pm2, \ldots$ is the sideband order, negative values corresponding to S frequencies.

For a flexural wave with axial propagation constant q and frequency Ω close to the cut-off frequency, which is given approximately by $\Omega_{\mathrm{co}} \approx (\pi/w)^2\sqrt{D/\sigma}$, we can use the Ansatz:

$$\delta(x,z,t) = \delta_0(x)\sqrt{\frac{e_{\mathrm{ac}}}{2\sigma\Omega_{\mathrm{co}}^2}}b(z,t)e^{i(qz-\Omega t)} + \text{c.c.}, \tag{5}$$

where $\sigma = \rho h$ is the mass per unit area of a web, e_{ac} is the acoustic energy per unit length in the axial direction, $\delta_0(x)$

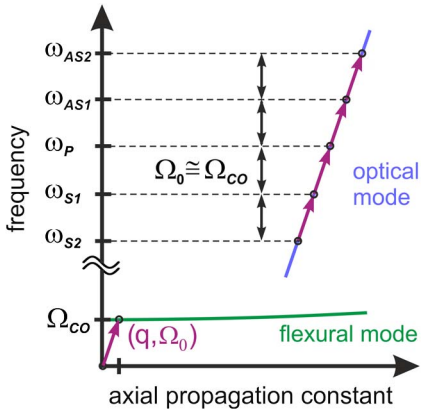

Fig. 4. Schematic of the dispersion diagram for SRLS by guided flexural waves with a cut-off angular frequency Ω_{co}. A phonon with frequency $\Omega_0 \approx \Omega_{\mathrm{co}}$ and propagation constant q automatically provides phase matching between successive optical S and AS components.

is the transverse profile of the flexural resonance (with units $m^{-1/2}$) normalized so that $\int_{-w/2}^{w/2} |\delta_0(x)|^2 dx = 1$, and $b(z,t)$ is the dimensionless slowly varying envelope of the flexural mode. The transverse profile has been taken for simplicity to be $\delta_0(x) = (2/w)^{1/2}\cos(\pi x/w)$, which approximates to its shape at the cut-off frequency. Substituting this expression into Eq. (3) in the absence of any driving terms and assuming exponential decay of sinusoidal oscillation in time yields a decay rate $\Gamma = \tau\Omega_{co}^2$.

Note that, although q is non-zero in the experiment, it is very small, taking the value $q = \beta_p - \beta_S \approx 2\pi f_{ac} n_m/c = 0.15\ m^{-1}$ for acoustic frequency $f_{ac} = 6$ MHz and modal index $n_m = 1.2$. This yields an axial acoustic wavelength of ~42 m, i.e., much longer than the fiber sample. Thus, in Eq. (3), we can assume that the z derivative of the deflection is negligibly small compared to its x derivative.

Now we apply the slowly varying envelope approximation to Eqs. (1) and (3), considering only those components of the optical driving term that oscillate with the same frequency and wavevector as the acoustic wave. Since the group velocity of the guided flexural wave at $\Omega_0 \approx \Omega_{co}$ is nearly zero (Fig. 4), we can neglect phonon propagation, i.e., set $\partial b/\partial z \approx 0$, and obtain the following set of coupled equations:

$$\frac{\partial a_n}{\partial z} + \frac{1}{v_g}\frac{\partial a_n}{\partial t} = i\kappa(b a_{n-1} + b^* a_{n+1}),$$
$$\frac{\partial b}{\partial t} + \left(\frac{\Gamma}{2} + \frac{\Omega^2 - \Omega_0^2}{2i\Omega}\right) b = i\gamma \sum_n a_n a_{n-1}^* + \xi_L, \quad (6)$$

where $v_g = \partial\omega/\partial\beta$ is the group velocity of the light (which is effectively identical for every frequency component) and ξ_L is the rate of seeding by Langevin noise, which is related to the forcing term in Eq. (3) via $\tilde{f} = -i\Omega\xi_L\zeta\exp(i(qz-\Omega t)) + \text{c.c.}$, where ζ and the other parameters in Eq. (6) are defined in Appendix A.

By eliminating $b(z)$ from Eqs. (6), the evolution of the fields can be rewritten for exact phase matching ($\Omega = \Omega_0$) and in the steady-state ($\partial/\partial t = 0$) for time-averaged values of all quantities as follows:

$$\frac{\partial a_n}{\partial z} = \frac{g_0 P_0}{2}\left(-a_{n-1}\sum_l a_l a_{l-1}^* + a_{n+1}\sum_l a_{l-1} a_l^*\right) + i\frac{2\kappa}{\Gamma}(\xi_L^{n-1} a_{n-1} + \xi_L^{n+1} a_{n+1}),$$
$$g_0 = \frac{4\kappa\gamma}{\Gamma P_0} = \frac{\omega_0 Q_{om}^2}{n_m c^2 h_p \sigma \Omega_0 \Gamma}\frac{\partial n_m}{\partial \delta}. \quad (7)$$

Since the frequency spacing between different optical comb lines and the spectral width of the comb in the experiment are much smaller than the carrier frequency of the pump wave, we have approximated ω_n by ω_0 for all n. The uncorrelated Langevin noise terms ξ_L^{n-1} and ξ_L^{n+1} (causing coupling to a_n from the lower- and higher-frequency sidebands) have the same statistics and are calculated anew for each realization of the code.

To quantify the gain factor g_0, we calculate the overlap between the optical mode and the flexural mode, using the numerical technique described in [11] and considering the geometry of the experimental structure. This results in $n_m = 1.24$, $\partial n_m/\partial\delta = -64\times10^3\ m^{-1}$ at the center of the optical mode, $h_p = -6.8\times10^{-6}$ m, and $Q_{om} = 661\ m^{-1/2}$. Further, we take the area density $\sigma = 10^{-3}\ kg/m^2$, the experimental values of the mechanical resonance frequency $\Omega_0 = 2\pi\times6.022$ MHz and linewidth $\Gamma \approx 1$ kHz, and calculate the gain coefficient at $\lambda = 1.55\ \mu m$ to be $g_0 \approx 10^6\ m^{-1}\,W^{-1}$. This exceeds the SRLS gain in small-core PCF [8] by six orders of magnitude.

4. DISCUSSION

The data points in Fig. 5 represent the measured powers in each optical sideband (normalized to the total power) at several different values of launched power. A pronounced threshold is observed at ~4.9 mW, which is not observed in numerical solutions of Eq. (7), which show that the sidebands begin to grow immediately even at infinitesimal power levels.

To explain the existence of the oscillation threshold in the experiment, we have found it necessary to consider acoustic mode competition in the system, by analogy with cavity mode competition in lasers. As mentioned before, structural nonuniformities are known to exist along the fiber. These will cause the appearance of many acoustic resonances, each with a slightly different frequency, localized at different positions along the fiber (see Fig. 3). Since all these resonances interact with the same guided optical mode and have similar gain characteristics, they destructively interfere, suppressing the SRLS process as long as the input power stays below a critical value.

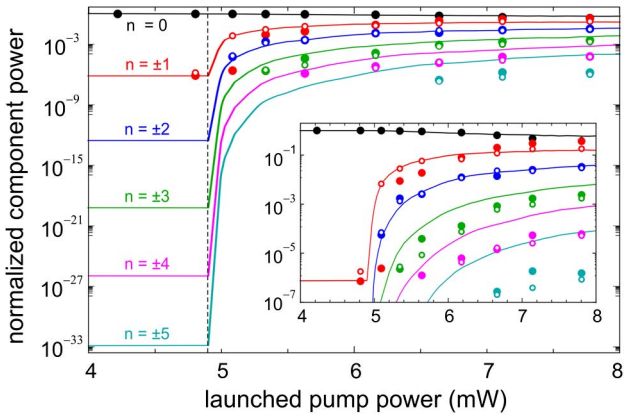

Fig. 5. Evolution of the power in the comb lines (normalized to the total output power) as a function of the launched pump power. Full and open circles represent experimental data for the S and AS components, respectively. Full lines show the theoretical expectations for the pump (black), the first-order (red), second-order (blue), third-order (green), fourth-order (magenta), and fifth-order (cyan) S and AS using the fit parameters $g_0 = 4\times10^6\ m^{-1}\,W^{-1}$ and an effective comb generation length $L_{eff} = 6$ cm. A distinct threshold for the onset of frequency comb generation occurs at a launched power of ~4.9 mW, marked by the dashed vertical line. Below threshold, the power in each comb line decreases exponentially with its order. The inset shows the experimentally relevant data range above a noise floor of $\sim10^{-7}$ relative to the pump power.

In our model we assume that, due to the Lorentzian lineshape of the gain profile, there is a power-dependent line narrowing that gradually reduces the overlap between competing acoustic modes. Above the critical power, the overlap is weak enough and the mode competition eliminated, so that a subset of the localized acoustic modes switches from random motion with zero mean phonon amplitude to coherent vibration with finite mean phonon amplitude. Thus, the effective nonlinear interaction length L_{eff} increases and consecutive optical sidebands are generated and amplified via SRLS.

The theoretical plots in Fig. 5 (solid lines) were obtained by numerically solving a model for acoustic mode competition and calculating the average from a set of 1000 different realizations seeded by stochastic acoustic noise. Good quantitative agreement with the experimental data is obtained using $g_0 = 4 \times 10^6\ \text{m}^{-1}\,\text{W}^{-1}$ and $L_{\text{eff}} = 6$ cm as the effective nonlinear length. Given the uncertainties in the values of acoustic linewidth and L_{eff}, the agreement between the theoretical and experimental values of gain is good. Due to the resolution limit of the measurement, the estimated acoustic linewidth (1 kHz) is likely to be too high, leading to an underestimate of the experimental gain. Also, uncertainty in L_{eff} leads to uncertainty in the value of g_0, since only the product $g_0 L_{\text{eff}}$ can be measured experimentally.

Finally, we address the appearance of secondary frequency combs around each primary sideband at pump powers above ~8 mW [Fig. 2(d)]. These arise from the presence of a second localized resonance at a slightly different frequency, caused by nonuniformities in the nanoweb structure (we have recently observed this using a side-scattering technique, to be reported elsewhere). This second resonance has a higher threshold power and acts on all the frequency components of the primary comb, so that each of the primary sidebands (spaced by $f_1 = 6.022$ MHz) pumps a secondary comb with a slightly different frequency spacing ($f_2 = 6.061$ MHz), resulting in the generation of a multiplicity of finely spaced frequencies $f = f_0 + nf_1 + mf_2$. As the spacing of the secondary comb is 39 kHz larger than that of the primary comb, the fine structure of the comb lines is offset by $n(f_2 - f_1) = n \times 39$ kHz from the center of the nth primary sideband. The remarkably high gain factor of SRLS results in full energy transfer from the primary fifth S and AS signals to the secondary comb lines at a pump power of 10.2 mW. An extended theory (to be published in detail elsewhere), including acoustic mode competition and dual-comb generation, confirms this picture.

5. CONCLUSIONS

A mechanically highly compliant nanostructure, consisting of two very thin glass membrane waveguides, experiences strong optical gradient forces when light is launched into it. The resulting mechanical deformation results in a large increase in effective modal phase index, i.e., a giant optomechanical nonlinearity. As a result, when the structure is pumped with CW laser light at the few-milliwatts level, it behaves like an artificial Raman-active molecule, causing the generation of a frequency comb with spacing equal to the acoustic resonant frequency.

This is the first time that single-pass stimulated Raman-like scattering, seeded from noise, has been observed in a nanomechanical resonator. By using thicker and less-wide webs, resonant frequencies as high as a few hundred megahertz seem possible (albeit with lower gain), suggesting that the structure may be useful in optical frequency metrology, spectroscopy, and passive mode locking of fiber lasers.

APPENDIX A

The constants in Eq. (6) are the rate of coupling per unit length between the optical frequency components

$$\kappa = \frac{\omega_0}{2c}\frac{\partial n_m}{\partial \delta} Q_{\text{om}} \sqrt{\frac{2e_{\text{ac}}}{\sigma \Omega_0^2}} \tag{A1}$$

and the rate of coupling per unit time from the optical beat note to the acoustic resonance

$$\gamma = \frac{\varepsilon_0 Z_0 P_0 Q_{\text{om}}}{2h_p n_m \sqrt{2\sigma e_{\text{ac}}}}, \tag{A2}$$

where

$$Q_{\text{om}} = \int_{-w/2}^{w/2} \delta_0(x)|s(x)|^2 \mathrm{d}x \tag{A3}$$

is the optomechanical overlap integral and h_p is a characteristic length given by [18]

$$h_p = (|f(y_{\text{upper}})|^2 - |f(y_{\text{lower}})|^2)^{-1}, \tag{A4}$$

where y_{upper} and y_{lower} are the positions of the upper and lower boundaries of a single nanoweb.

The statistics of the Langevin noise seeding rate ξ_L in Eq. (6) are defined as [21]

$$\langle \xi_L(z,t) \rangle = 0 \quad \text{and}$$
$$\langle \xi_L(z,t)\xi_L^*(z',t') \rangle = \frac{k_B T}{e_{\text{ac}}} \Gamma \delta(z-z')\delta(t-t'). \tag{A5}$$

Here, k_B denotes Boltzmann's constant and T is the ambient temperature. These expressions are used to stochastically initiate the system in the numerical simulations.

Finally, the parameter ζ used to relate $\tilde{f}$ to ξ_L takes the form

$$\zeta = \frac{\sqrt{2\sigma e_{\text{ac}}}}{\Omega_0}\left(\int_{-w/2}^{w/2} \delta_0(x)\mathrm{d}x\right)^{-1} = \frac{\pi}{2\Omega_0}\sqrt{\frac{\sigma e_{\text{ac}}}{w}}. \tag{A6}$$

Note that this expression applies only to the fundamental flexural mode.

FUNDING INFORMATION

Max Planck Society

REFERENCES

1. R. Riviere, S. Deleglise, S. Weis, E. Gavartin, O. Arcizet, A. Schliesser, and T. J. Kippenberg, "Optomechanical sideband cooling of a micromechanical oscillator close to the quantum ground state," Phys. Rev. A **83**, 063835 (2011).
2. A. H. Safavi-Naeini, J. Chan, J. T. Hill, T. P. M. Alegre, A. Krause, and O. J. Painter, "Observation of quantum motion of a nanomechanical resonator," Phys. Rev. Lett. **108**, 033602 (2012).
3. M. Aspelmeyer, T. J. Kippenberg, and F. Marquardt, "Cavity optomechanics," arXiv:1303.0733v1 (2013).
4. P. Dainese, P. St.J. Russell, G. S. Wiederhecker, N. Joly, H. L. Fragnito, V. Laude, and A. Khelif, "Raman-like light scattering from acoustic phonons in photonic crystal fiber," Opt. Express **14**, 4141–4150 (2006).
5. G. Bahl, J. Zehnpfennig, M. Tomes, and T. Carmon, "Stimulated optomechanical excitation of surface acoustic waves in a microdevice," Nat. Commun. **2**, 403 (2011).
6. W. H. P. Pernice, M. Li, and H. X. Tang, "A mechanical Kerr effect in deformable photonic media," Appl. Phys. Lett. **95**, 123507 (2009).
7. D. Van Thourhout and J. Roels, "Optomechanical device actuation through the optical gradient force," Nat. Photonics **4**, 211–217 (2010).
8. M. S. Kang, A. Nazarkin, A. Brenn, and P. St.J. Russell, "Tightly trapped acoustic phonons in photonic crystal fibres as highly nonlinear artificial Raman oscillators," Nat. Phys. **5**, 276–280 (2009).
9. M. S. Kang, N. Y. Joly, and P. St.J. Russell, "Passive mode-locking of fiber ring laser at the 337th harmonic using gigahertz acoustic core resonances," Opt. Lett. **38**, 561–563 (2013).
10. A. Butsch, M. S. Kang, T. G. Euser, J. R. Koehler, S. Rammler, R. Keding, and P. St.J. Russell, "Optomechanical nonlinearity in dual-nanoweb structure suspended inside capillary fiber," Phys. Rev. Lett. **109**, 183904 (2012).
11. A. Butsch, C. Conti, F. Biancalana, and P. St.J. Russell, "Optomechanical self-channeling of light in a suspended planar dual-nanoweb waveguide," Phys. Rev. Lett. **108**, 093903 (2012).
12. J. R. Koehler, A. Butsch, T. G. Euser, R. E. Noskov, and P. St.J. Russell, "Effects of squeezed-film damping on the optomechanical nonlinearity in dual-nanoweb fiber," Appl. Phys. Lett. **103**, 221107 (2013).
13. J. R. Koehler, A. Butsch, T. G. Euser, and P. St.J. Russell, "Frequency comb generation via optomechanical nonlinearity in evacuated dual-nanoweb fibre," in *Frontiers in Optics Conference*, (Optical Society of America, 2013), paper FTh3B.3.
14. D. Braje, L. Hollberg, and S. Diddams, "Brillouin-enhanced hyperparametric generation of an optical frequency comb in a monolithic highly nonlinear fiber cavity pumped by a cw laser," Phys. Rev. Lett. **102**, 193902 (2009).
15. P. Del'Haye, A. Schliesser, O. Arcizet, T. Wilken, R. Holzwarth, and T. J. Kippenberg, "Optical frequency comb generation from a monolithic microresonator," Nature **450**, 1214–1217 (2007).
16. M. D. Duncan, R. Mahon, J. Reintjes, and L. L. Tankersley, "Parametric Raman gain suppression in D_2 and H_2," Opt. Lett. **11**, 803–805 (1986).
17. O. E. DeLange, "Optical heterodyne detection," IEEE Spectrum **5**, 77–85 (1968).
18. C. Conti, A. Butsch, F. Biancalana, and P. St.J. Russell, "Dynamics of optomechanical spatial solitons in dual-nanoweb structures," Phys. Rev. A **86**, 013830 (2012).
19. A. N. Norris, "Flexural waves on narrow plates," J. Acoust. Soc. Am. **113**, 2647–2658 (2003).
20. L. D. Landau and E. M. Lifshitz, *Theory of Elasticity* (Butterworth-Heinemann, 1986).
21. R. W. Boyd and K. Rzazewski, "Noise initiation of stimulated Brillouin scattering," Phys. Rev. A **42**, 5514–5521 (1990).